Contribution from the School of Chemical Sciences,
University of Illinois at Urbana-Champaign, Urbana, Illinois 61801

Electron Paramagnetic Resonance Study of Intermolecular Exchange Coupling in an Undiluted Vanadyl Complex[1]

GREGORY D. SIMPSON, R. LINN BELFORD,* and R. BIAGIONI

Received February 13, 1978

Pure crystals of *cis*-bis(1-phenyl-1,3-butanedionato)oxovanadium(IV) display anomalous fine structure in their EPR spectra; 13 or fewer distinct features appear depending upon orientation. The features originate in a combination of ^{51}V hyperfine structure with fine structure caused by dipolar and exchange coupling of nearest-neighbor molecules related by inversion through the unit cell origin. The spectra can be simulated to reasonable accuracy with coaxial **g** and **A** matrices, a spin–spin coupling tensor **D** based on point dipoles at the metal nuclei, a small ferromagnetic exchange coupling, and an orientation-dependent line width predicted by the Van Vleck dipolar broadening formula. The best-fit parameters are $g_\perp = 1.982$, $g_\parallel = 1.943$, $A_\parallel = -510$, $A_\perp = -210$, $D_{xx} = -7.92$, $D_{yy} = 143.85$, $D_{zz} = -130.53$, $D_{xz} = 201.90$, and $J = -540$ (A, D, and J in units of MHz). Both direct and indirect paths are available for the intersite exchange process, which corresponds to an exchange rate of $\sim 10^9$/s.

Introduction

This work is an outgrowth of our interests in the coordination chemistry of oxovanadium(IV)[2-13] and in the use of electron paramagnetic resonance both to characterize transition-metal ions[9-29] and to study interelectronic coupling between neighboring sites.[13-17]

Electron paramagnetic resonance has been used extensively in investigating bonding[30] and interactions[31] of transition-metal complexes. Among these metal complexes those of vanadium occupy a unique position due to the extreme stability of the VO^{2+} oxo ion.[32] Although there have been many EPR studies of oxovanadium systems, most have involved liquids or frozen solutions.[33] The possibility of single-crystal work is limited by the scarcity of suitable host lattices, although a few such studies have been reported.[10] Measurements on pure single crystals seldom yield much information on account of magnetic concentration. The many neighboring dipoles in the crystal split the resonance lines; consequently the spectrum is unusually broadened to such an extent that no hyperfine structure is resolved. (See, for example, ref 13.) Extended exchange interactions further degrade the spectra. However, there are rare examples of concentrated paramagnetic samples which display some fine structure. We have found such structure in an unusual pattern in pure crystalline *cis*-bis(1-phenyl-1,3-butanedionato)oxovanadium(IV), $VO(benzac)_2$. Hon, Belford, and Pfluger[2b] determined the crystal and molecular structure. The molecule can have cis and trans isomers; only the cis has been isolated to date. The crystals are monoclinic with four molecules per unit cell. The molecules are associated in inversion pairs as shown in Figure 1, with a vanadium–vanadium distance of 5.7 Å.

Here we report a study of the anomalous orientation- and temperature-dependent EPR spectra of single crystals of $VO(benzac)_2$. The unusual hyperfine structure and the anisotropic line widths are analyzed in terms of exchange and dipolar interactions. The associated large Hamiltonian matrix problem is solved by approximations described in the Appendix.

Experimental Section

The compound was prepared as reported previously.[2b] Elemental analysis of the powder gave the following results: % C calcd 61.33, found 61.7; % H calcd 4.58, found 4.66. The compound was recrystallized from acetone which had been boiled to remove oxygen. The air-sensitive solution was kept in a desiccator under its own vapor. Single crystals suitable for X- and Q-band work grew in about a day.

EPR spectra of single crystals at room temperature were recorded at both X-band (~9.5 GHz) and Q-band (34.4 GHz)[34] frequencies with Varian E-9 and E-15 spectrometers. Also, Q-band spectra of a crystal at 77 K were recorded. The magnetic field was calibrated by proton resonance, and the frequencies were computed from the resonance line center of powdered DPPH ($g = 2.0036$). For X-band work a single crystal was oriented by X-ray precession methods and then transferred to a single-circle goniometer designed for the purpose. In this way the orientation was known to within about a degree.

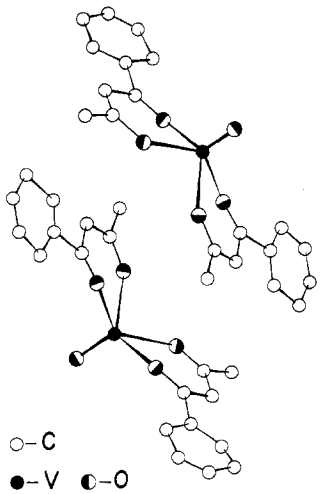

Figure 1. Skeletal structure of inversion pairs of vanadyl bis(benzoylacetonate). The vanadium–vanadium distance here is 5.7 Å.

For Q-band measurements the crystal was transferred to a small quartz rod protruding from the bottom plate of the EPR cavity. The uncertainty of orientation was greater here due to the method of placing the cavity in the magnetic field. However, comparison of the angular dependence of these spectra with that at X-band frequencies aided in assigning the orientations.

Computational analyses employed the IBM 360-75 and DEC-PDP 10 computers at the University of Illinois with programs written specifically for this problem (cf. Appendix). Simulated spectra were displayed on a Calcomp plotter.

Results

The marked orientational dependence of the experimental spectra is exhibited in Figure 2. At the orientation of maximum spectral width (~0.16 T) there are nine equally spaced peaks, the intensity of the two outermost derivative maxima being roughly half the intensity of the others. The overall width then decreases to a minimum (~0.06 T) at which no hyperfine structure is resolved. The nine-line pattern suggests that interaction between inversion pairs is of approximately the same magnitude as the hyperfine interaction. Oxovanadium complexes, in which the magnitude of these interactions is much less than the hyperfine interaction, exhibit spectra[35] with eight peaks of about equal intensity. For interactions the magnitude of which is much greater than that of the hyperfine interaction,[3] each electron is equally affected by both nuclei; therefore each is coupled to a quantized total

0020-1669/78/1317-2424$01.00/0

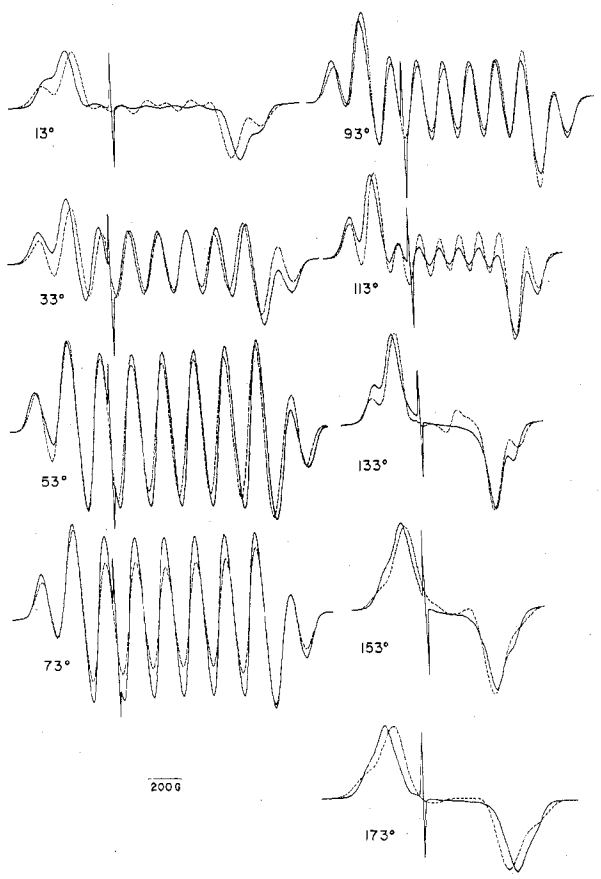

Figure 2. Orientational dependence of Q-band (34.4 GHz) EPR spectra of an undiluted single crystal of vanadyl bis(benzoylacetonate). Spectra were recorded in the a, c^* crystallographic plane. The solid lines are the experimental spectra. Simulations are given by the broken lines.

nuclear spin. The resulting 15 lines have relative intensities 1, 2, 3, 4, 5, 6, 7, 8, 7, 6, 5, 4, 3, 2, 1.

The Hamiltonian used for spectral simulations is given in eq 1, where S_1, I_1 and S_2, I_2 are spin operators for center 1

$$H = \beta B\eta\cdot\mathbf{g}\cdot S + h(S_1\cdot\mathbf{D}\cdot S_2 + S_1\cdot\mathbf{A}\cdot I_1 + S_2\cdot\mathbf{A}\cdot I_2 + JS_1\cdot S_2) \quad (1)$$

and center 2, respectively, of an exchange-coupled pair of vanadium centers. The 256 × 256 Hamiltonian matrix was prepared in a basis of simultaneous eigenvectors of S^2, S_z, I_z, and I_z' ($I_z' \equiv I_{z1} - I_{z2}$). Certain approximations considerably simplified the calculations. In particular, interactions between states of different M_s were neglected; see Appendix for details.

The molecular coordinate system was defined so that the vanadyl (V=O) bond is directed along the z axis, with x and y directions chosen so as to simplify the **D** tensor, i.e., to make $D_{xy} = D_{yz} = 0$. The molecular coordinate system is related to an orthonormal crystal coordinate system (with axes chosen to coincide with the crystallographic a, b, and c^* axes) by the direction cosines given in eq 2. The relationship between these

$$\begin{bmatrix} x \\ y \\ z \end{bmatrix} = \begin{bmatrix} -0.003011 & 0.937968 & -0.346706 \\ -0.862035 & 0.173292 & 0.476305 \\ 0.506839 & 0.300301 & 0.808039 \end{bmatrix} \begin{bmatrix} a \\ b \\ c^* \end{bmatrix} \quad (2)$$

two coordinate systems is shown in Figure 3. The angle between the magnetic field vector and the a axis in the a, c^* plane (the molecules are magnetically equivalent in this plane) is denoted as ρ.

A comparison of simulated with experimental spectra for various orientations is shown in Figure 2. These spectra show that the effective hyperfine splitting reaches a maximum for

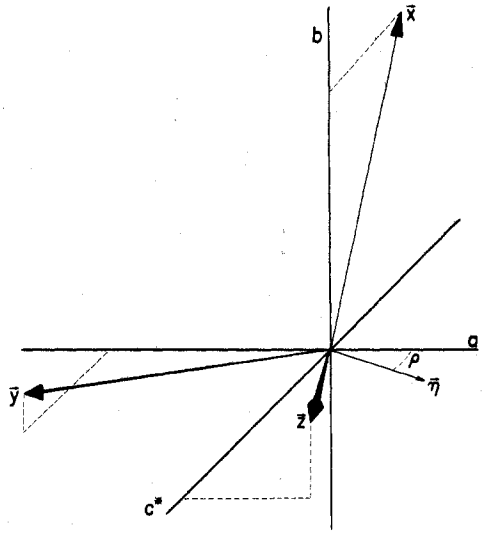

Figure 3. The relationship between the molecular (x, y, z) coordinate system and the orthonormal coordinate system (a, b, c^*). The orientation of the magnetic field vector, η, is given by ρ, with 0° being along the a axis and the positive sense of rotation toward c^*.

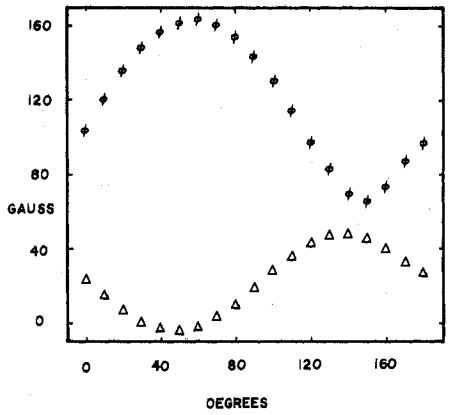

Figure 4. A comparison of effective dipolar splitting, Δ, with effective hyperfine splitting, ϕ, in crystalline vanadyl bis(benzoylacetonate). The effective dipolar splitting was calculated by a point dipole–point dipole model with spins located at the nearest-neighbor vanadium nuclei.

$\rho = 60°$. At this angle the magnetic field vector is closest to the molecular z axis ($\theta = 17°$). The minimum hyperfine spacing occurs when the magnetic field vector passes through the molecular x, y plane ($\rho = 150°$).

Examination of the unusual spectral structure suggests a dipolar and/or exchange interaction. Previous calculations[36] showed the dipolar interaction to have approximately the right magnitude but the wrong orientational dependence to explain this structure. By means of a point dipole model, with electron spins located at the vanadium nuclei, we have calculated the effective dipolar splitting for each orientation. Elements of the **D** tensor calculated in the molecular coordinate system are $D_{xx} = -0.000\,264$, $D_{yy} = 0.004\,795$, $D_{zz} = -0.004\,351$, and $D_{xz} = -0.006\,730$ cm^{-1}. A rotation about the y axis gives a diagonal **D** matrix, the elements of which are $D_1 = 0.004\,276$, $D_2 = 0.004\,795$, and $D_3 = -0.009\,341$ cm^{-1}. The g anisotropy prevents this matrix from being traceless. A comparison of the effective dipolar splitting with effective hyperfine splitting is shown in Figure 4. At the point of maximum hyperfine splitting the dipolar splitting has just reached a minimum. Clearly, the additional splitting needed to give the unusual structure cannot be the result of a pure dipolar interaction. Addition of an exchange interaction of comparable magnitude and correct sign alters the predicted orientational dependence.

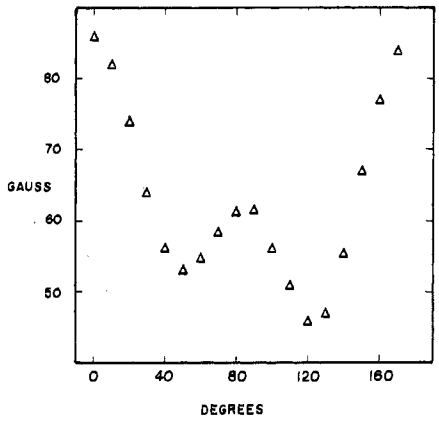

Figure 5. The effective line width due to interaction of a vanadium nucleus with other vanadium nuclei other than the inversion twin in an undiluted crystal of vanadyl bis(benzoylacetonate). The line width was estimated by use of Van Vleck's dipolar broadening formula.

Attempts to simulate spectra with an empirical isotropic line width were unsuccessful for spectra like that for $\rho = 173°$. Therefore, an anisotropic line width contributed by dipolar interaction with dipoles of neighboring pairs was introduced. Positions of all dipoles in all the unit cells which border and include a particular unit cell were calculated. Then the effective line width, ΔB, was estimated through Van Vleck's dipolar broadening formula[37] (eq 3). Here g is the g factor,

$$(\Delta B)^2 = \frac{3}{4}g^2\beta^2 S(S+1)\sum_{j,k}\frac{(1 - 3\cos^2\theta_{jk})^2}{r_{jk}^6} \qquad (3)$$

β is the Bohr magneton, r_{jk} is the distance between the jth and kth dipoles, and θ_{jk} is the angle between r_{jk} and the magnetic field vector. This orientational dependence is shown in Figure 5. The maximum in the dipolar line broadening occurs for $\rho = 0°$ (i.e., $B||a$) because neighbors are spaced closely along the a axis.

The set of parameters listed provided very good simulations of the experimental spectra. Because of the many approximations employed, we would not expect, and did not find, any one set of parameters to fit all spectra perfectly. The simulations generally deteriorated when any parameter was outside the given range.

$$g_{\parallel} = 1.943 \pm 0.001$$

$$g_{\perp} = 1.982 \pm 0.001$$

$$A_{\parallel} = -510 \pm 30 \text{ MHz } (-0.0170 \pm 0.0010 \text{ cm}^{-1})$$

$$A_{\perp} = -210 \pm 15 \text{ MHz } (-0.0070 \pm 0.0005 \text{ cm}^{-1})$$

$$J = -540 \pm 45 \text{ MHz } (-0.0180 \pm 0.0015 \text{ cm}^{-1})^{38}$$

$$D_{xx} = -7.91 \text{ MHz } (-0.000\,264 \text{ cm}^{-1})$$

$$D_{yy} = 143.75 \text{ MHz } (+0.004\,795 \text{ cm}^{-1})$$

$$D_{zz} = -130.44 \text{ MHz } (-0.004\,351 \text{ cm}^{-1})$$

$$D_{xz} = -201.90 \text{ MHz } (-0.006\,730 \text{ cm}^{-1})$$

Discussion

Our success in simulating the spectra indicates that the interactions of this system occur mainly between the two molecules related by inversion; interactions with other molecules affect only the line width. The principal interaction within each inversion pair is exchange.

We were able to determine not only the magnitude of J but also its sign because J and D are of similar magnitude. The sign of the exchange interaction is revealed by its interplay with the effective dipolar splitting. The exchange is ferromagnetic in nature ($J < 0$); i.e., the ground state is a triplet, the singlet lying 0.018 cm^{-1} above it. In favorable cases such as this, exchange values of this small magnitude can be readily determined by EPR methods but not by the usual magnetic susceptibility techniques.

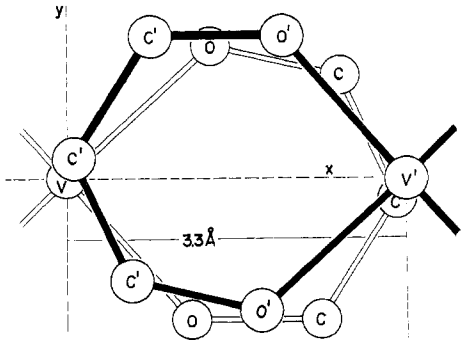

Figure 6. An orthogonal projection of part of an inversion pair of vanadyl bis(benzoylacetonate) onto the molecular x, y plane. The $d_{x^2-y^2}$ orbitals of the two vanadium nuclei have lobes which are directed toward the projection of the other in this plane. One vanadium lies 4.5 Å out of this plane; the other lies in the plane.

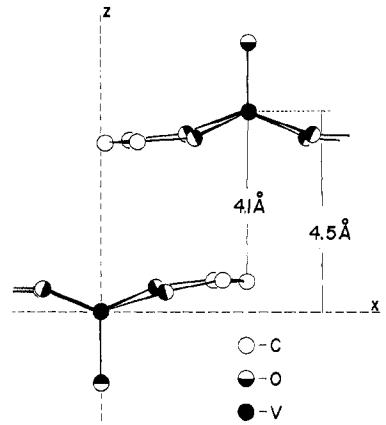

Figure 7. An orthogonal projection of part of an inversion pair of vanadyl bis(benzoylacetonate) onto the molecular x, z plane. The two rings shown are parallel and situated favorably for the interaction of their π systems. The nearest carbon–vanadium distance here is 4.1 Å.

Exchange interactions within dimers have received a great deal of study.[39,40] Both direct[41-43] (i.e., metal orbital–metal orbital overlap) and indirect[44,45] (the so-called superexchange) exchange mechanisms are well established. The structure of $VO(benzac)_2$ prevents a clear-cut decision between these two mechanisms. Figure 6 shows an orthogonal projection of an inversion pair onto the molecular x, y plane. The unpaired electron resides in the $d_{x^2-y^2}$ orbital; the relationship between the $d_{x^2-y^2}$ orbitals of the two centers is shown. Center 2 lies about 4.5 Å out of the plane. The $d_{x^2-y^2}$ orbitals of the two centers will overlap to some extent in the vicinity of the inversion center (2.8 Å from each V atom). Even though the radial distribution function for this orbital is small for large values of r, the observed magnitude of the exchange interaction is so small that direct overlap cannot be ruled out. Similarly, a superexchange mechanism is possible. Figure 7 shows an orthogonal projection of an inversion pair onto the molecular x, z plane. The relationship between one vanadium-containing ring of a molecule and the vanadium atom of its inversion twin is shown. This ring and its inversion partner are fairly close (3.4 Å), parallel, and situated favorably for interaction of their π systems (see also Figure 6). The nearest carbon–vanadium distance is about 4.1 Å. Exchange interaction could occur

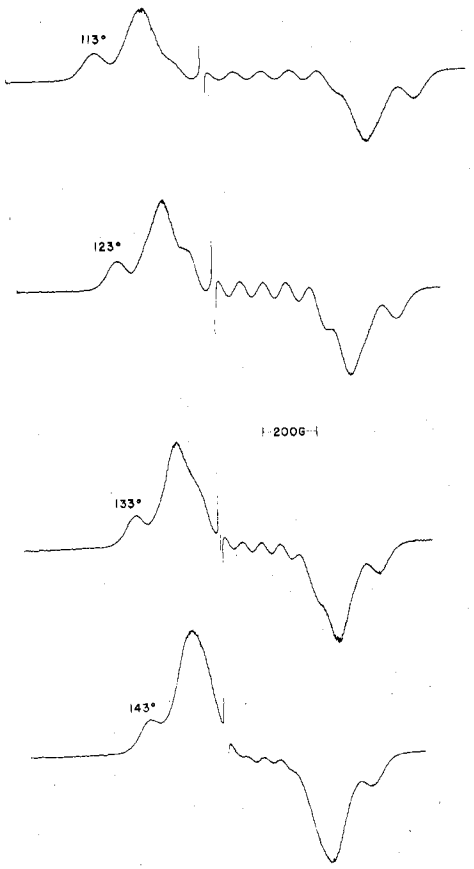

Figure 8. Q-band (34.6 GHz) EPR spectra at 77 K of an undiluted single crystal of vanadyl bis(benzoylacetonate) for several orientations of magnetic field in the *a*, *c** plane. Note that at one orientation, $\rho = 123°$, ten distinct features are resolved.

through the π–π interaction path. Note that in this system the chelate rings are not in the *x*, *z* plane, and the metal d_{xz} orbitals are not orthogonal to the π orbitals of the chelate rings; there is an indirect path.

Most studies of exchange coupling have employed systems with much smaller metal–metal distances, but there are several reports of small exchange coupling. For example, Davis and Belford[16] found $J = 0.0050$ cm^{-1} for Cr^{3+}–Cr^{3+} pairs having a nearest neighbor distance of approximately 7 Å. Meredith and Gill[46] and Svare and Seidel[48] determined $J = 0.034$ and $J = 0.045$ cm^{-1}, respectively, for Cu^{2+}–Cu^{2+} exchange-coupled pairs having large center-to-center distances. James and Luckhurst[47] and Hasegawa, Yamada, and Miura[50] found low *J* values for two binuclear vanadyl tartrate complexes in solution, although the exact nature of each of these species was not well-known. For the much larger exchange coupling constants of more tightly linked copper systems, Hatfield[51] obtained a rough relationship between the Cu–O–Cu angle and exchange value. Until further magnetic studies of oxovanadium systems with known structures can be done, any discussion relating structure to exchange value would be inordinately speculative.

Extended exchange interaction throughout the $VO(benzac)_2$ crystal is probably much less than that in similar complexes of copper(II) because in the vanadyl system the unpaired electron resides in a nonbonding orbital which is rather localized. In contrast, the unpaired electron in a corresponding copper(II) system would reside in an antibonding (d_{xy}) orbital which would interact more strongly with the ligand rings and provide a more efficient mechanism for extended magnetic interactions in the crystal. Magnetic concentration should be much more severe in copper(II) than in vanadyl crystals. We expect that studies such as this one could be carried out on several vanadyl systems.

In an attempt to see more detailed structure, we also recorded spectra of an oriented $VO(benzac)_2$ crystal at 77 K and 35 GHz (see Figure 8). Although there was no further resolution of each hyperfine line, these spectra show modified splitting patterns with up to ten lines. This further splitting we attribute to an increase in both $|J|$ and $|D|$ caused by contraction of the crystal. Davis and Belford[16] used temperature variation to study internuclear-distance-dependence of exchange for a system involving Cr^{3+}–Cr^{3+} pairs. In the absence of low-temperature structural data, which would provide a priori values for the elements of the dipolar splitting matrix, the large line widths involved here would make such a determination very difficult for $VO(benzac)_2$.

Acknowledgment. We thank Dr. Michael Valek and Professor N. Dennis Chasteen for preliminary studies of this problem and Mr. Kevin Klotter for obtaining some preliminary spectra. The U.S. National Institute of General Medical Sciences, National Science Foundation, and the donors of the Petroleum Research Fund, administered by the American Chemical Society, provided support.

Appendix

A computer program was written to construct and approximately diagonalize the spin Hamiltonian (eq 1) which contains the electronic spin operators for the two electrons (S_1 and S_2) and the nuclear spin operators (I_1 and I_2) for the two vanadium nuclei. The matrix representation of the Hamiltonian took a convenient form when reexpressed in terms of sum and difference operators.

$$H = \beta B\eta\cdot\mathbf{g}\cdot S + (S\cdot\mathbf{A}\cdot I + S'\cdot\mathbf{A}\cdot I')/2 + (S\cdot\mathbf{D}\cdot S - S'\cdot\mathbf{D}\cdot S')/4 + J(S\cdot S - S'\cdot S')/4$$

where $S = S_1 + S_2$, $I = I_1 + I_2$, $S' = S_1 - S_2$, and $I' = I_1 - I_2$.

The appropriate 256×256 matrix operators were built by direct-product operations upon the smaller individual-particle spin matrices (i.e., the 2×2 matrices for each electronic spin and the 8×8 matrices for each nuclear spin). Electronic spin matrices were developed in the four-dimensional electronic spin space (i.e., $\{\mathbf{S}_1\}_{4\times4} = \mathbf{S}_{2\times2} \otimes \mathbf{1}_{2\times2}$, $\{\mathbf{S}_2\}_{4\times4} = \mathbf{1}_{2\times2} \otimes \mathbf{S}_{2\times2}$). Similarly, nuclear spin matrices were developed in the 64-dimensional nuclear spin space (i.e., $\{\mathbf{I}_1\}_{64\times64} = \mathbf{I}_{8\times8} \otimes \mathbf{1}_{8\times8}$; $\{\mathbf{I}_2\}_{64\times64} = \mathbf{1}_{8\times8} \otimes \mathbf{I}_{8\times8}$). Finally, nuclear and electronic spin operators were directly multiplied as prescribed by the terms of the spin Hamiltonian to provide the 256×256 full-matrix representation. The electronic Zeeman term was diagonalized by a similarity transformation. In general three Euler angles (α, β, γ) are required for this transformation, but if the molecule possesses axial symmetry[49] only two are required. A proper choice of the third simplifies the Hamiltonian matrix. The choice of $\gamma = 0$ causes A_{xy} and A_{yz} to vanish and eliminates all the imaginary parts of the hyperfine interaction matrices.

The full Hamiltonian matrix takes the form shown.

$$\begin{bmatrix} \mathbf{G} + \mathbf{D}_1 + \mathbf{J} + \mathbf{A}_1 & -\mathbf{A}_2' & \mathbf{A}_2 + \mathbf{D}_4 & \mathbf{D}_3 \\ & -(\mathbf{D}_1 + \mathbf{D}_2) & \mathbf{A}_1' & \mathbf{A}_2' \\ & & \mathbf{D}_2 - \mathbf{D}_1 + \mathbf{J} & \mathbf{A}_2 - \mathbf{D}_4 \\ & & & -\mathbf{G} + \mathbf{D}_1 + \mathbf{J} - \mathbf{A}_1 \end{bmatrix}$$

$$\mathbf{G} = \mathbf{g}\beta B \times \mathbf{1}_{64\times64}$$

$$\mathbf{A}_1 = \tfrac{1}{2}(A_{zz}\mathbf{I}_z + A_{xz}\mathbf{I}_x)$$

$$\mathbf{A}_2 = \tfrac{1}{2}2^{1/2}(A_{xx}\mathbf{I}_x + A_{xz}\mathbf{I}_z - iA_{yy}\mathbf{I}_y)$$

$$\mathbf{D}_1 = D_{zz}/4 \times \mathbf{1}_{64\times64}$$

$$\mathbf{D}_2 = \tfrac{1}{4}(D_{xx} + D_{yy}) \times \mathbf{1}_{64\times64}$$

$$\mathbf{D}_3 = \tfrac{1}{4}(D_{xx} - 2D_{xy} - D_{yy}) \times \mathbf{1}_{64\times64}$$

$$\mathbf{D}_4 = (2^{1/2}/8)(D_{xz} - iD_{yz}) \times \mathbf{1}_{64\times64}$$

$$\mathbf{J} = J \times \mathbf{1}_{64\times64}$$

Primed elements indicate that $\mathbf{I}'$ matrices are to replace $\mathbf{I}$ for that particular element.

An exact solution of this large 256 × 256 matrix (each block represents a 64 × 64 matrix) for each orientation of the crystal in the magnetic field and for each set of trial parameters would be both costly and time consuming (the cost of diagonalizing a matrix is proportional to the cube of its order). The use of perturbation methods is complicated by the fact that, excluding the electronic Zeeman term, there is no clear-cut hierarchy of operations; i.e., dipolar, hyperfine, and exchange interactions are similar in magnitude. Therefore, another approach based on matrix partitioning was developed. The Hamiltonian matrix was set up to allow second-order perturbation corrections associated with elements connecting $M_s = \pm1$ and 0 blocks, but those corrections proved unnecessary. The electronic Zeeman term is the dominant term in this matrix. Levels belonging to different M_s are separated by an amount significantly greater than any of the levels within a given M_s; therefore, only a small error is introduced by neglecting 64 × 64 blocks connecting different M_s levels. The 256 × 256 matrix is reduced to a 64 × 64 real, symmetric, banded matrix (there are two, but the same set of eigenvectors diagonalize both) and a 128 × 128 matrix. By forming an eigenvalue equation and making use of the special form of this 128 × 128 matrix, one can find its eigensystem by rapid diagonalization of a single real, symmetric, banded 64 × 64 matrix, **M**.

$$\begin{bmatrix} a \times \mathbf{1}_{64\times64} & \mathbf{M} \\ \mathbf{M} & b \times \mathbf{1}_{64\times64} \end{bmatrix} \begin{bmatrix} u \\ v \end{bmatrix} = \begin{bmatrix} u \\ v \end{bmatrix} \begin{bmatrix} \ddots & & \\ & \lambda & \\ & & \ddots \end{bmatrix}$$

Here a and b are constants. With **M** in diagonal form, the eigenvalues are simply roots of quadratic equations. The form of the matrix which diagonalizes the entire 256 × 256 Hamiltonian, aside from off-diagonal blocks connecting states of different M_s, follows:

$$\begin{bmatrix} & R_1{}^{\mathrm{T}}R_{21} & R_1{}^{\mathrm{T}}R_{22} & \\ R_{21}{}^{\mathrm{T}}R_1 & & & R_{21}{}^{\mathrm{T}}R_1 \\ R_{22}{}^{\mathrm{T}}R_1 & & & R_{22}{}^{\mathrm{T}}R_1 \\ & R_1{}^{\mathrm{T}}R_{21} & R_1{}^{\mathrm{T}}R_{22} & \end{bmatrix}$$

where R_{22} and R_{21} are proportional to the matrix of eigenvectors of **M**, and R_1 is the matrix of eigenvectors which diagonalize the $M_s = \pm1$ 64 × 64 matrices. Transition intensities were computed by the standard formula

$$T_{nm} = |\langle n|\eta_{osc}\cdot\boldsymbol{g}\cdot S|m\rangle|^2$$

where η_{osc} is the unit vector of the oscillating microwave magnetic field.

Registry No. $VO(benzac)_2$, 60133-41-7.

References and Notes

(1) Material taken in part from the B.S. thesis of R. Biagioni, 1974, and the Ph.D. thesis of G. D. Simpson, 1978, University of Illinois, Urbana.
(2) (a) G. Basu, W. A. Yeranos, and R. L. Belford, *Inorg. Chem.*, **3**, 929 (1964); (b) P. K. Hon, R. L. Belford, and C. E. Pfluger, *J. Chem. Phys.*, **43**, 1323 (1964).
(3) R. E. Tapscott and R. L. Belford, *Inorg. Chem.*, **6**, 735 (1967).
(4) R. E. Tapscott, R. L. Belford, and I. C. Paul, *Inorg. Chem.*, **7**, 356 (1968).
(5) B. H. Bersted, R. L. Belford, and I. C. Paul, *Inorg. Chem.*, **7**, 1557 (1968).
(6) N. D. Chasteen, R. L. Belford, and I. C. Paul, *Inorg. Chem.*, **8**, 408 (1969).
(7) R. E. Tapscott, R. L. Belford, and I. C. Paul, *Coord. Chem. Rev.*, **4**, 323 (1969).
(8) M. H. Valek, W. A. Yeranos, G. Basu, P. K. Hon, and R. L. Belford, *J. Mol. Spectrosc.*, **37**, 228 (1971).
(9) M. A. Hitchman, C. D. Olson, and R. L. Belford, *J. Chem. Phys.*, **50**, 1195 (1969).
(10) M. A. Hitchman and R. L. Belford, *Inorg. Chem.*, **8**, 958 (1969).
(11) M. A. Hitchman, B. W. Moores, and R. L. Belford, *Inorg. Chem.*, **8**, 4817 (1969).
(12) R. L. Belford, D. T. Huang, and H. So, *Chem. Phys. Lett.*, **14**, 592 (1972).
(13) R. L. Belford, N. D. Chasteen, H. So, and R. E. Tapscott, *J. Am. Chem. Soc.*, **91**, 4675 (1969).
(14) R. L. Belford, R. J. Missavage, I. C. Paul, N. D. Chasteen, W. E. Hatfield, and J. F. Villa, *Chem. Commun.*, 508 (1971).
(15) R. L. Belford, P. H. Davis, G. G. Belford, and T. M. Lenhardt, *ACS Symp. Ser.*, **No. 5**, 40 (1974).
(16) P. H. Davis and R. L. Belford, *ACS Symp. Ser.*, **No. 5**, 51 (1974).
(17) C. J. Doumit, G. L. McPherson, S. B. Lanoux, J. B. Jonassen, and R. L. Belford, *Inorg. Chem.*, **16**, 565 (1977).
(18) B. W. Moores and R. L. Belford in "Electron Resonance of Metal Complexes", T. F. Yen, Ed., Plenum Press, New York, N.Y., 1969, Chapter 2.
(19) M. A. Hitchman and R. L. Belford, ref 18, Chapter 7.
(20) H. So and R. L. Belford, *J. Am. Chem. Soc.*, **91**, 2392 (1969).
(21) H. So and R. L. Belford, *Phys. Rev. B*, **2**, 3810 (1970).
(22) P. H. Davis and R. L. Belford, *Inorg. Chem.*, **10**, 1557 (1971).
(23) R. L. Belford and J. R. Pilbrow, *J. Magn. Reson.*, **11**, 381 (1973).
(24) P. H. Davis, L. K. White, and R. L. Belford, *Inorg. Chem.*, **14**, 1753 (1975).
(25) L. K. White and R. L. Belford, *Chem. Phys. Lett.*, **37**, 553 (1976).
(26) L. K. White and R. L. Belford, *J. Am. Chem. Soc.*, **98**, 4428 (1976).
(27) M. Nilges, R. L. Belford, E. K. Barefield, and P. H. Davis, *J. Am. Chem. Soc.*, **99**, 755 (1977).
(28) B. Harrowfield, J. R. Pilbrow, and R. L. Belford, *J. Magn. Reson.*, **28**, 433 (1977).
(29) N. D. Chasteen and R. L. Belford, *Inorg. Chem.*, **9**, 169 (1970).
(30) B. R. McGarvey, *Transition Met. Chem.*, **3**, 89 (1966).
(31) G. F. Kokoszka and R. W. Duerst, *Coord. Chem. Rev.*, **5**, 209 (1970).
(32) J. Selbin, *Coord. Chem. Rev.*, **1**, 293 (1966).
(33) H. A. Kuska and M. T. Rogers in "Radical Ions", E. T. Kaiser and L. Kevan, Ed., Interscience, New York, N.Y., 1959, pp 579–745.
(34) Q-band instrument settings were as follows: scan range = 2000 G, field set = 12 500 G, time constant = 0.03/s, scan time = 2 min, modulation amplitude = 20 G, modulation frequency = 100 kHz, receiver gain = 20, microwave power = 22 mW.
(35) R. Wilson and D. Kivelson, *J. Chem. Phys.*, **44**, 154 (1966).
(36) M. Valek, D. Chasteen, and R. L. Belford, unpublished results.
(37) J. H. Van Vleck, *Phys. Rev.*, **74**, 1168 (1948).
(38) Our convention regarding J is as follows. With the singlet at zero energy, the triplet lies J energy units above the singlet for $J > 0$. The triplet is the ground state for $J < 0$.
(39) T. D. Smith and J. R. Pilbrow, *Coord. Chem. Rev.*, **13**, 173 (1974).
(40) W. E. Hatfield, *Inorg. Chem.*, **11**, 216 (1972), and ref 3–22 cited therein.
(41) B. N. Figgis and R. L. Martin, *J. Chem. Soc.*, 3837 (1956).
(42) I. B. Ross, *Trans. Faraday Soc.*, **55**, 105 (1959).
(43) A. P. Ginsberg, E. Koubek, and H. J. Williams, *Inorg. Chem.*, **5**, 1656 (1966).
(44) P. W. Anderson in "Magnetism", Vol. 1, G. Rado and H. Suhl, Ed., Academic Press, New York, N.Y., 1963, pp 25–83.
(45) W. E. Hatfield and J. S. Paschal, *J. Am. Chem. Soc.*, **86**, 3888 (1964).
(46) D. J. Meredith and J. C. Gill, *Phys. Lett. A*, **25**, 429 (1967).
(47) P. G. James and G. R. Luckhurst, *Mol. Phys.*, **18**, 141 (1970).
(48) I. Svare and G. Seidel, *Phys. Rev.*, **134**, A172 (1964).
(49) The assumption of axial symmetry is a good one; see ref 4.
(50) A. Hasegawa, Y. Yamada, and M. Miura, *Bull. Chem. Soc. Jpn.*, **44**, 3335 (1971).
(51) W. E. Hatfield, *ACS Symp. Ser.*, **No. 5**, 108 (1974).